

# Identification of Pressed Keys by Time Difference of Arrivals of Mechanical Vibrations

Gerson de Souza Faria<sup>a,1,\*</sup>, Hae Yong Kim<sup>a,1</sup>,

<sup>a</sup>*Departamento de Engenharia de Sistemas Eletrônicos, Escola Politécnica, Universidade de São Paulo, Av. Prof. Luciano Gualberto, tr. 3, 158, CEP 05508-010, São Paulo, Brazil*

---

## Abstract

The possibility of finding the sequence of pressed keys in a mechanical keyboard is a serious security threat. In our previous work, we have shown that it is possible to identify, with high probability, the pressed key by analyzing the vibration generated by the keystrokes. At that time, we did not know the physical phenomenon responsible for leaking information as mechanical vibration. In this paper, we show that the TDOA (Time Difference of Arrivals) of the mechanical waves is the main culprit for leaking information. To demonstrate this hypothesis, we glued three accelerometers in a PIN-pad, collected the vibrations generated by the keystrokes and computed the relative delays of vibration arrival times in pairs of accelerometers. We show that it is possible to estimate the positions of the keys through simple difference of the delays. A simple classification scheme using the delays yielded 96.4% of recognition success rate. The same technique can be used to attack devices with touch-sensitive screen, identifying the region touched.

---

## 1. Introduction

2 Mechanical keypads are widely used for entering confidential data. Confiden-  
3 tial passwords are typed in mechanical keypads in ATMs (Automatic Teller Ma-  
4 chines) or PIN-pads (devices used in smart card transactions to input the card-

---

\*Corresponding author

*Email addresses:* [gerson.faria@usp.br](mailto:gerson.faria@usp.br) (Gerson de Souza Faria), [hae@lps.usp.br](mailto:hae@lps.usp.br) (Hae Yong Kim)

5 holder’s Personal Identification Number). In some countries, including Brazil,  
6 electors use electronic voting machines with mechanical keyboards to choose the  
7 candidate. Thus, the possibility that someone finds out the sequence of pressed  
8 keys, without the user’s knowledge or consent, is a serious security threat. In  
9 card operations, the theft of card information in an otherwise legitimate trans-  
10 action, known as “skimming”, was responsible for 87% of attacks against ATMs  
11 in 2013, as reported in [1].

12 In a previous work [2], we have shown that it is possible to identify the  
13 pressed key with high probability by gluing accelerometers in the device, ac-  
14 quiring acceleration signals generated by keystrokes and analyzing these signals.  
15 We called it “vibration attack”.

16 Usually, modern ATM keypads are encrypted. They are sealed modules that  
17 encrypt the PIN soon after the entry. So, non-encrypted PIN numbers are not  
18 meant to be accessible from outside either by physically tapping onto wires or re-  
19 motely sensing electromagnetic radiation. Any tampering of the keypad causes  
20 it to permanently disable itself. Similarly, PIN-pads are protected modules that  
21 permanently disable themselves if tampered. The possibility of identifying the  
22 sequence of pressed keys through mechanical vibrations is a serious security fail-  
23 ure of secure keypads because they are designed to resist against any attempt of  
24 eavesdropping. The devices will continue functioning normally while passwords  
25 are stolen.

26 When we wrote our previous paper, we did the experiments without knowing  
27 the physical phenomenon responsible for the leak of information. We extracted  
28 a lot of features from the vibration signals (up to 165 features per keystroke)  
29 and fed machine learning algorithms with them in an attempt to identify the  
30 pressed key. This was enough to certify the existence of the problem, but without  
31 a satisfactory explanation of the underlying phenomenon.

32 In this work, we show that the propagation delay of the transverse wave  
33 generated by the keystroke is the main phenomenon responsible for the infor-  
34 mation leaking. With this knowledge, in this work we use much less features per  
35 keystroke (2 instead of up to 165) and less training data (100 or 200 keystrokes

36 per experiment instead of up to 2400 keystrokes) and obtain similar classifica-  
37 tion success rates than in our earlier work. This result is somewhat surprising,  
38 because PIN-pad is far from being a homogeneous medium, and one would ex-  
39 pect that the vibration propagation velocities were different in different regions  
40 of the device. To provide our technique a short name, we will call it “vibration  
41 delay attack”.

42 It is also possible to estimate the position of the pressed key (the source of  
43 the wave) through a simple 2-D trilateration of the relative delays of the signals  
44 captured by the accelerometers. This is a well known technique in a variety  
45 of fields by terms like TDOA (Time Difference of Arrivals) or simply “time of  
46 flight”. For instance, the accurate measurement of these delays is the basis of  
47 GPS (Global Positioning System) and other geolocation systems. Geophysicists  
48 and seismologists also use it in order to locate the epicenters of earthquakes and  
49 of other seismic events [3]. In our case, the position of the key is analogous to  
50 the epicenter of an earthquake.

51 In the literature, there are some papers that identify the pressed key by  
52 sound, because each key usually emits a characteristic sound when pressed.  
53 Asonov and Agrawal [4] achieved 79% of key recognition success rate when  
54 identifying one out of 30 keys in a PC keyboard. Berger *et al.* [5] use keyboard  
55 acoustic emanations and a dictionary to recognize correctly 73% of the English  
56 words typed in a PC keyboard, without any training. Zhuang *et al.* [6] takes as  
57 input 10-minute sound recording of a user typing English text using a keyboard  
58 and recovers up to 96% typed characters. Halevi [7] uses keyboard acoustic  
59 emanations for eavesdropping over random passwords, without using dictionary,  
60 achieving 40% to 64% recognition rate per character.

61 Similarly to acoustic emission, each key seems to emit a characteristic me-  
62 chanical vibration when pressed. However, this idea has been much less explored  
63 in the literature. Marquardt and Verma [8] use this idea to recognize keystrokes  
64 of a computer keyboard. They use the accelerometer of a smartphone placed  
65 near the computer’s keyboard to capture the vibrations. They do not actually  
66 identify the pressed key. Instead, they classify keystrokes in “left” or “right” and

67 pairs of keystrokes in “near” and “far”. They achieved classification rates from  
68 65% to 91% making those binary decisions.

69 The phenomenon identified in this work is of a different nature: even if it  
70 were possible to have all the keys emit exactly the same sound and the same  
71 mechanical vibration, it would be still possible to identify the pressed key by  
72 the arrival times of the vibration wave. Our purpose in this work is neither to  
73 select the most appropriate classifier nor to achieve extremely high recognition  
74 rates. Instead, our primary aim is to show that there is one more physical  
75 phenomenon that can be used to identify the pressed key by means of a simple  
76 location technique, but applied in a complex non-homogeneous medium. Most  
77 of location experiments use relatively homogeneous solids, like concrete, metal,  
78 glass, acrylic etc. and not composite ones, like a PIN-pad. We use in all  
79 experiments only the relative delays as features and a simple Naive Bayesian  
80 classifier. If we add other features and fine-tune the classifier, probably we would  
81 achieve higher success rates. Additionally, our finding also opens the possibility  
82 of attacking touch-screen devices, because the same phenomenon occurs when  
83 the user interacts with them. Note that touch-screen devices cannot be attacked  
84 using acoustic emanations.

85 The literature on trilateration comes from diverse fields of research. Maochen  
86 Ge discusses the source location theories and methods that are used for earth-  
87 quake, microseismic and acoustic emission [9, 10]. He analyzes the principles  
88 of source location methods and mentions the main causes of inaccuracy, for  
89 instance, imprecision of sensor positions and errors in arrival time measur-  
90 ing. Geolocation methods based on measuring the time difference of arrivals  
91 (TDOAs) of signals received from several geostationary satellites are presented  
92 in [11, 12, 13]. Ho and Chan present a method that solves a set of nonlinear  
93 equations to estimate the location [11]. Gustafsson and Gunnarsson compare a  
94 Monte Carlo method and a gradient search algorithm [12]. Schumacher *et al.*  
95 propose a Bayesian approach for the problem of source location in the materials  
96 research [14]. Arun *et al.* [15] develop a location method based on Kullback-  
97 Leibler discrimination information criteria on spectra of acceleration signals,

98 testing the method on a large aluminium plate.

99 The rest of the paper is organized as follows. Basic theory on transverse  
100 waves is described in Section 2. We apply the vibration delay attack in two de-  
101 vices: a simple mockup keypad in Section 3 and a commercial PIN-pad designed  
102 to be secure in Section 4. We make some considerations comparing the previous  
103 results with the new ones in Section 5 and present our conclusions in Section 6.  
104 Appendixes present the definition of normalized cross correlation (used to esti-  
105 mate the relative delay between two signals) and the source location estimation  
106 method.

## 107 2. Vibration of a Plate

### 108 2.1. Theory

109 The behavior of a transverse wave in a bar or plate (with thickness) is consid-  
110 erably more complex than the classical transverse wave in a string or membrane  
111 (with negligible thickness). Plates and bars have thickness, bringing properties  
112 as bending stiffness (also known as flexural rigidity) defined as the resistance  
113 offered by the plate while undergoing bending or deflection.

114 The differential equation for the deflection of a one-dimensional string is [16]:

$$\nabla^2 y(x, t) = \frac{1}{c^2} \frac{\partial^2 y(x, t)}{\partial t^2}, \quad c^2 = \frac{T}{\rho} \quad (1)$$

115 where  $T$  is the tension and  $\rho$  is the mass density of the material. All functions  
116 of the form  $y(x, t) = F_1(x - ct) + F_2(x + ct)$ ,  $\forall F_1, F_2$ , are its solutions, where  $c$   
117 is the constant velocity of the traveling wave without shape deformation.

118 On the other hand, the simplified wave equation for the transverse vibration  
119 of a uniform bar is:

$$\nabla^4 y(x, t) = -\frac{1}{a^2} \frac{\partial^2 y(x, t)}{\partial t^2}, \quad a^2 = \frac{EI}{m} \quad (2)$$

120 where  $E$  is the modulus of elasticity of the material,  $I$  is its moment of inertia  
121 and  $m$  its total mass. Let us assume that a solution of Eq. 2 is a simple harmonic  
122 wave traveling with velocity  $v$ :

$$y(x, t) = A \cos \frac{2\pi}{\lambda} (x - vt) \quad (3)$$

123 Substituting Eq. 3 in Eq. 2, we obtain a velocity that depends on the wavelength,  
124  $v = a \frac{2\pi}{\lambda}$ . Note in the previous relation that  $a$  does not possess dimensions of  
125 velocity, so it does not represent a velocity, instead of  $c$  in Eq. 1 that is in fact  
126 a velocity.

127 In summary, the travelling velocity of a wave is constant in a string but,  
128 in a bar, it depends on the wavelength and consequently on the oscillation  
129 frequency, because the latter is a *dispersive medium*. A sinusoidal wave can  
130 travel in a dispersive medium without suffering deformation in its shape, but  
131 a wave packet will be deformed in such a medium since its components have,  
132 by construction, distinct wavelengths. In this case, each component will travel  
133 with a distinct velocity thus causing deformation [16, 17].

134 The same phenomenon occurs in plates, like the acrylic plate where we made  
135 the two initial experiments (Sections 2.2 and 3).

136 The dispersion and reflections make it difficult to accurately measure the  
137 delays in the arrival of mechanical vibrations, because different ways of pressing  
138 keys generate distinct spectra and so different delays between wavefronts and  
139 reflection occurrences. We measure the delays of wavefronts considering them  
140 as packets travelling with a group velocity. The group velocity of a wave is the  
141 velocity with which the overall shape of the wave's amplitudes propagates.

## 142 2.2. Dispersion in Acrylic Plate

143 In order to observe in practice the effect of medium dispersion and group  
144 velocity presented in Section 2.1, we made an experiment in an acrylic plate  
145 using two distinct sources of excitation: (i) touching the plate with the finger  
146 and (ii) touching it with the tip of a mechanical pencil. Fig. 1 depicts the  
147 assembly of the experiment. The dimensions of the plate are approximately  
148 3mm×640mm×670mm. We mounted the two accelerometers over small metallic  
149 screws and glued them on the acrylic plate.  $A_1$  and  $A_2$  are the positions of the  
150 accelerometers.

151 In all the experiments, we use Freescale MMA7361 analog triaxial low-g  
152 accelerometers [18] operating in  $\pm 1.5g$  range and a Tektronix TDS-2004B digital

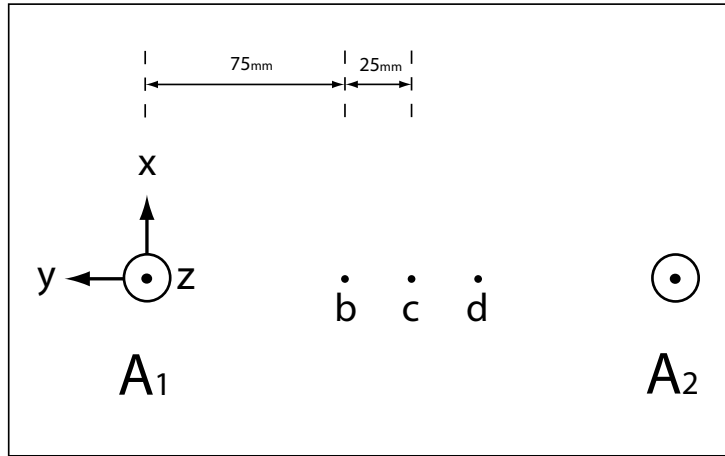


Figure 1: Assembly of the experiment to observe the medium dispersion in acrylic plate.

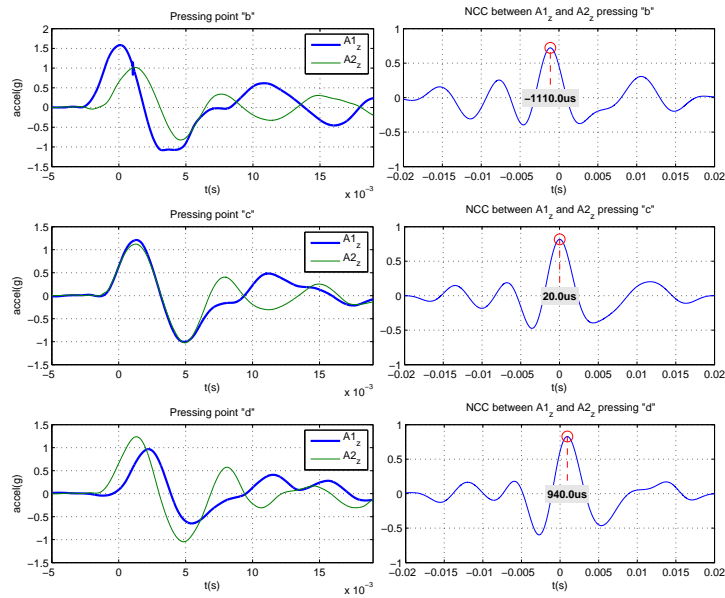


Figure 2: (Left) Acceleration signals obtained tapping the acrylic plate with finger at points 'b', 'c' and 'd'. (Right) Relative delay estimated using the position of the highest peak in NCC between  $A1_z$  and  $A2_z$ .

153 oscilloscope to acquire the data. Each signal vector comprises 2500 points, the  
 154 maximum allowed by the oscilloscope. The sampling rate varies from experiment

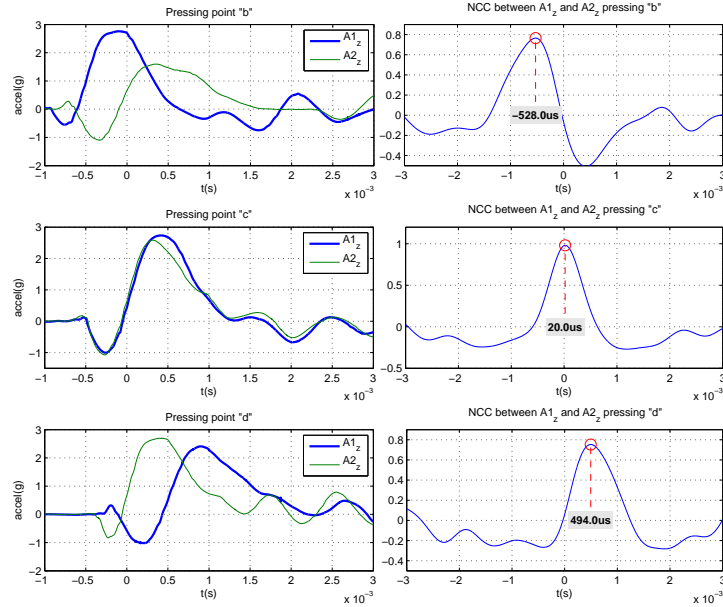


Figure 3: (Left) Acceleration signals obtained tapping the acrylic plate with a mechanical pencil at points ‘b’, ‘c’ and ‘d’. (Right) Relative delay estimated using the position of the highest peak in NCC between  $A1_z$  and  $A2_z$ .

155 to experiment. In this case, the sampling rate was 100KS/s for the experiment  
 156 touching the plate with the finger and 500KS/s for touching it with a mechanical  
 157 pencil.

158 The left column of Fig. 2 depicts the transverse  $\vec{z}$  acceleration signals ac-  
 159 quired by the accelerometers, touching the plate with the finger at points “b”, “c”  
 160 and “d”. Longitudinal waves in  $\vec{x}$  and  $\vec{y}$  directions are much faster than trans-  
 161 verse waves because they travel inside the material and not on its surface. So,  
 162 we ignored the longitudinal signals, processing only surface transverse signals  $\vec{z}$ .

163 Obviously, a wavefront in a homogeneous and isotropic medium arrives first  
 164 at the nearest accelerometer. Thus, the wavefront arrives first at  $A_1$  when  
 165 touching the point “b”. The wave arrives first at  $A_2$  touching point “d”. The  
 166 wavefront reaches simultaneously at the two accelerometers pressing the middle  
 167 point “c”.



168 *2.3. Delay estimation via NCC*

169 We use normalized cross correlation (NCC) to compute the relative delay  
170 between the signals acquired by the two accelerometers (see Appendix A for the  
171 definition and computation of NCC). Suppose that the wavefront generated by  
172 a keystroke takes  $n_1$  sampling periods to reach the accelerometer  $A_1$  and takes  
173  $n_2$  sampling periods to reach the accelerometer  $A_2$  (see Fig. 2). In this case, we  
174 will observe a peak in NCC between the acceleration values obtained by  $A_1$  and  
175 those obtained by  $A_2$ , when the latter is shifted right  $n_1 - n_2$  positions. This  
176 difference is the estimated delay.

177 The right column of Fig. 2 depicts the NCC between the signals acquired  
178 by the two accelerometers touching the acrylic plate with the finger. Using the  
179 peaks in NCC we computed the group velocity, that was estimated as  $\approx 45\text{m/s}$ .  
180 Fig. 3 depicts the signals obtained and the NCC touching the plate with the tip  
181 of a mechanical pencil. The group velocity is more than twice faster,  $\approx 95\text{m/s}$ ,  
182 because the frequency generated touching the plate with the pencil is higher  
183 than touching it with the finger.

184 The duration of the first semi-cycle of the signal  $A_{1z}$  tapping with the finger  
185 (Fig. 2) is  $\approx 5\text{ms}$ , corresponding to frequency of  $\approx 100\text{Hz}$  (if considered cyclic).  
186 The duration of the first semi-cycle of the signal  $A_{1z}$  tapping with the pencil  
187 (Fig. 3) is  $\approx 1\text{ms}$ , corresponding to frequency of  $\approx 500\text{Hz}$  (if considered cyclic).

188 **3. Acrylic Plate Mockup Keypad**

189 We constructed a mockup keypad using an acrylic plate to verify if the  
190 vibration delay can be used to identify the pressed key. We fixed a paper print  
191 of a keypad on the plate (Fig. 4), glued three accelerometers and touched inside  
192 each region emulating the keys. If we achieve a high accuracy in this test, it  
193 would be worth continuing the tests in real devices. We pressed 10 times each  
194 one of “0” to “9” virtual keys, generating 100 acquisitions.

195 Fig. 5 (top) depicts a typical keystroke captured by the three accelerometers.  
196 These signals are complex due to dispersion, reflections and many other wave

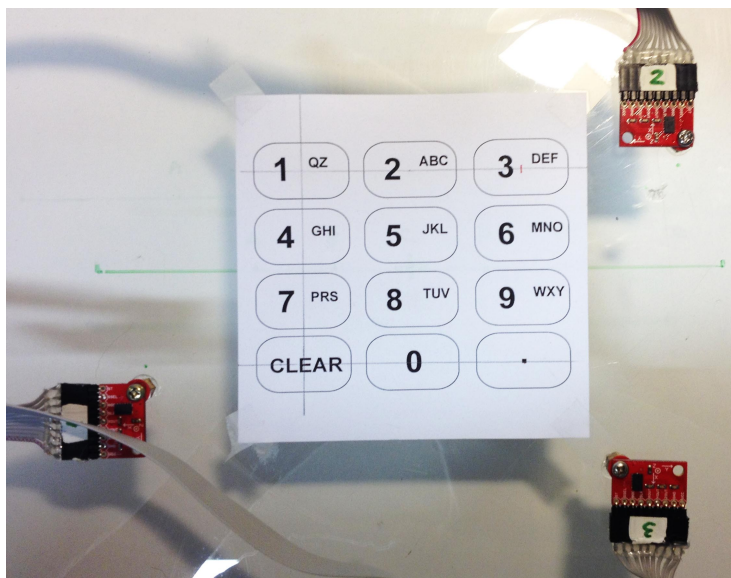


Figure 4: Keypad emulation on an acrylic plate. We tapped inside each virtual key to emulate keystrokes.

197 phenomena. So, if we simply compute the NCC between a pair of these signals,  
 198 the highest peak may not correspond to the relative delay. It is possible to  
 199 remove the artifacts introduced by the reflections by analyzing only the first  
 200 points in time of the signal, before the arrival of the reflections. To this end,  
 201 we enveloped the signals with a Gaussian window with mean  $\mu$  and standard-  
 202 deviation  $\sigma$ . We compute the highest peak in the first  $M$  points in each of the  
 203 three original signals and then set  $\mu$  as the average position of the three peaks,  
 204 as shown in Fig. 5. The parameters  $\sigma$  and  $M$  depend on the experiment.

205 In this experiment, the sampling rate was 25KS/s or 50KS/s. We used  
 206  $\sigma = \frac{200}{\sqrt{2}}$  for sampling rate of 25KS/s and  $\sigma = \frac{100}{\sqrt{2}}$  for 50KS/s, and  $M = 1500$   
 207 for both.

208 After multiplying the three original signals with the Gaussian window, we  
 209 take pairs of the enveloped signals and compute NCC between each pair. The  
 210 position of the highest peak in NCC is considered the relative delay between the  
 211 pair. As we have three original signals, we get three relative delays. However, we

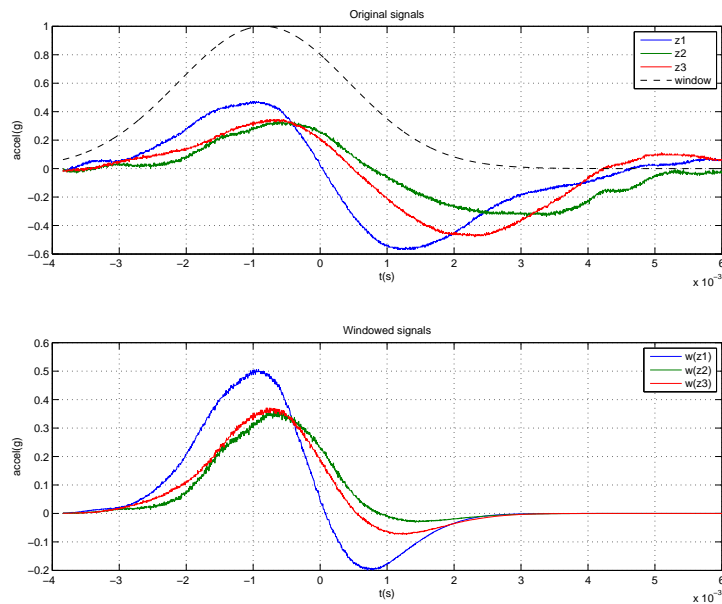


Figure 5: We apply a Gaussian window to attenuate the reflections and improve the delay estimation. (Top) the original acceleration signals took from the PIN-pad experiment, key “8”. (Bottom) the windowed signals.

212 noted that only two out of these three relative delays are independent features,  
 213 because the third can be obtained as a linear combination of the first two. See  
 214 Appendix B for explanation.

215 In our previous paper [2], we extracted up to 165 features from each keystroke,  
 216 instead of only two. The features were the values of NCC (instead of the po-  
 217 sition of the highest peak in NCC). In our very preliminary conference paper  
 218 [19], we used many tentative features before choosing NCC. At those times,  
 219 we made these choices because we had no clear idea of the underlying physical  
 220 phenomenon.

221 We use in all experiments a simple Naive Bayes classifier with normal dis-  
 222 tribution. We took randomly 80% of all features as the training set and 20% as  
 223 the test set, repeat this procedure 100 times and present the classification result  
 224 as a confusion matrix.

225 In this “mockup keypad” experiment, we obtained 100% of correct classifi-

Table 1: Confusion Matrix of the Acrylic Plate Mockup Keypad Experiment

Key	1	2	3	4	5	6	7	8	9	0
1	200									
2		200								
3			200							
4				200						
5					200					
6						200				
7							200			
8								200		
9									200	
0										200

226 cation rate (Table 1)! Evidently, this is an ideal situation. In order to visualize  
 227 spatially the data, we used 2-D trilateration (Appendix B) to estimate the rel-  
 228 ative locations of keys (Fig. 6). The estimated positions closely resemble their  
 229 actual positions. Moreover, the clusters of keys are clearly separated. This  
 230 shows that the group velocity is constant throughout the acrylic plate, because  
 231 it is a homogeneous and isotropic medium as we assumed in the source local-  
 232 ization method.

#### 233 4. PIN-pad

234 After the experiment with the acrylic plate, we applied the vibration delay  
 235 attack to a PIN-pad designed to deal with sensitive information in a secure way.  
 236 Fig. 7 shows the device, an Ingenico iPP320 PIN-pad and the assembly of the  
 237 experiment, where the three accelerometers were glued inside the SAM (Secure  
 238 Access Module) card access compartment. This device is PCI-PTS compliant<sup>1</sup>,  
 239 under 2.X and 3.X versions.

<sup>1</sup> PCI stands for Payment Card Industry. PTS stands for PIN Transaction Security, a set of requirements specific for PIN entry devices. Device compliance can

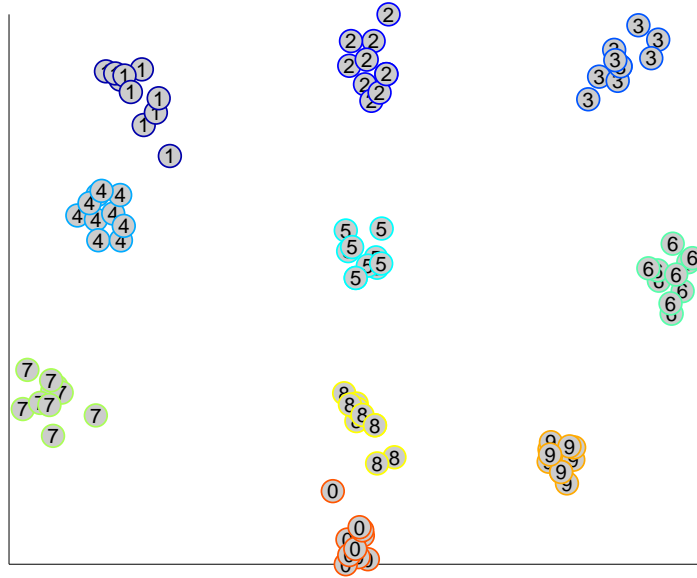


Figure 6: Estimation of the key positions of the acrylic keypad experiment.

240 The choice of this model/brand was not guided by any prior vulnerability  
 241 we could spot. We want to make it clear that most of PIN-pads with a SAM  
 242 card compartment are potential targets of this attack and Ingenico’s iPP320 is  
 243 not a special case.

244 The SAM card compartment increases the vulnerability to vibration delay  
 245 attack mainly because:

- 246 1. it provides room for implanting wiretap devices or “bugs”, hidden within  
 247 the compartment;
- 248 2. the compartment is normally located just below the keypad, the ideal  
 249 place to capture the vibrations from the keystrokes;
- 250 3. the SAM slots can eventually provide electrical power for the “bugs”.

---

be consulted at [https://www.pcisecuritystandards.org/approved\\_companies\\_providers/approved\\_pin\\_transaction\\_security.php](https://www.pcisecuritystandards.org/approved_companies_providers/approved_pin_transaction_security.php)



Figure 7: (a) PIN-pad used in the experiment with approximate locations of accelerometers. (b) The bottom view showing the SAM compartment with the implanted accelerometers.

251 Thus, the attack can be executed in real scenario in a noninvasive and unde-  
 252 tectable way, without batteries and wires. We placed the accelerometers inside  
 253 the SAM card compartment to simulate a real vibration delay attack. In a real  
 254 attack, however, miniaturized bug devices may be placed inside this compart-  
 255 ment.

256 The restricted space in the SAM card compartment does not allow us to  
 257 place the accelerometers wherever we want. So, the triangle formed by the  
 258 three accelerometers covered only a small portion of the area where the keys  
 259 are located (Fig. 7 (a)). We used spacers between the device’s chassis and the  
 260 printed circuit boards of the accelerometers, to make the accelerometers feel the  
 261 vibration of only a small area, hoping that this may improve the results.

262 We pressed 20 times each one of the “0” to “9” keys. As before, we enveloped  
 263 the three signals with a Gaussian window with  $\sigma = \frac{450}{\sqrt{2}}$  and  $M = 1500$ . We  
 264 used sampling rate of 250KS/s.

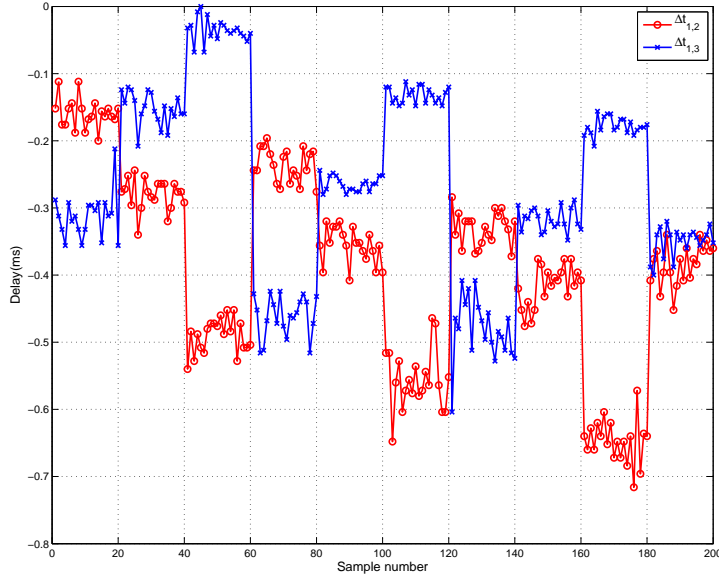


Figure 8: The features obtained in PIN-pad experiment. Each graph represents the delays between pairs of signals. X-axis is the test number, that is,  $x = 1$  to 20 correspond to key “1”,  $x = 21$  to 40 to key “2” and  $x = 181$  to 200 to key “0”. Only  $\Delta t_{1,2}$  and  $\Delta t_{1,3}$  were used. See text.

265 *4.1. Features*

266 Fig. 8 depicts the obtained features. Each graph represents the delays be-  
 267 tween the signals obtained by a pair of accelerometers. The  $x$  coordinate indi-  
 268 cates the test number. For example,  $x = 1$  to 20 correspond to the 20 strokes  
 269 of key “1”,  $x = 21$  to 40 to key “2” and  $x = 181$  to 200 to key “0”. As before, we  
 270 used only two features,  $\Delta t_{1,2}$  and  $\Delta t_{1,3}$ .

271 Table 2 shows the confusion matrix. The recognition rate is very high  
 272 ( $96.4 \pm 6\%$ ), where 6 is the standard deviation of the 100 cross validations. The  
 273 errors occur only between the neighboring keys. Moreover, excluding the key  
 274 “0” (that seems to be a special case) the errors occur only between neighboring  
 275 keys that belong to the same column. We observed similar results in [2]. Our  
 276 hypothesis is that this happens because the distance between columns ( $\approx 23\text{mm}$ )  
 277 is almost twice the distance between rows ( $\approx 13\text{mm}$ ), making it easier to make

Table 2: Confusion Matrix of the Pin-pad Experiment

Key	1	2	3	4	5	6	7	8	9	0	Acc.(%)
1	400										100.0
2		398			2						99.5
3			400								100.0
4				400							100.0
5					397		3				99.2
6						382		18			95.5
7							389		11		97.2
8								345	55		86.2
9									400		100.0
0							5	50		345	86.2

278 row misclassifications.

279 In this experiment, the reconstruction of the key locations is also very good  
280 (Fig. 9) though the clusters are not so clearly separated as in the ideal case  
281 (Section 3). The keys are uniformly distributed in space with the exception of  
282 keys “0” and “8” that are partially mixed (in agreement with the confusion matrix  
283 in Table 2 and features in Fig. 8). These results show that the supposition of  
284 constant group velocity used in the source location method (Appendix B) is  
285 reasonable in practice, in spite of the apparent complexity of the medium. The  
286 observed localization errors may be due to: (a) the triangle formed by the  
287 accelerometers covers only a small part of the keypad; (b) the group velocity  
288 may not be constant throughout all the device; (c) the delay estimation method  
289 is not accurate enough; and (d) the medium is dispersive.

#### 290 4.2. From NCC to TDOA

291 The instant of the peak in NCC can be used to estimate the delay between  
292 two similar signals (Section 2.3). In a previous work [2], we used the amplitudes  
293 of NCC as features to identify the pressed keys, without computing the instant  
294 of the peak. This implied large feature vectors (up to 165 features), as opposed  
295 to small TDOA features here used (only 2 features). However, the dimension



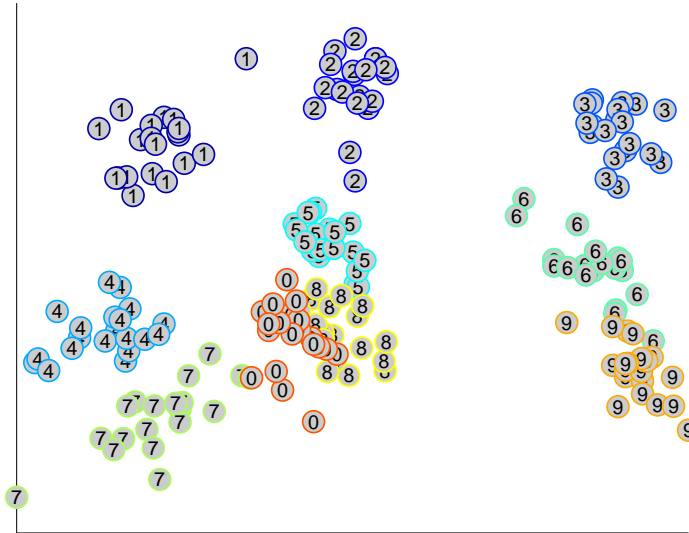


Figure 9: Estimation of the key locations of the PIN-pad experiment.

296 of NCC features can be reduced using some standard dimensionality reduction  
 297 technique, as PCA (Principal Component Analysis). We used PCA to reduce  
 298 NCC amplitudes into two main features. Fig. 10 shows that the two features so  
 299 obtained are very well-correlated with the TDOA features we used throughout  
 300 this paper. This clearly demonstrates the delay of arrival is the main physical  
 301 phenomenon that identifies the pressed key.

302 Feeding the Bayes learning algorithm with the two features obtained by  
 303 NCC-PCA, the obtained recognition rate was 95.1%, very close to the 96.4%  
 304 obtained with the TDOA features. Using the three most important features  
 305 obtained by NCC-PCA, the recognition rate is 97.7%, slightly higher than the  
 306 rate obtained with the two TDOA features. This may indicate that there are  
 307 other information (besides the time of arrival) in the NCC amplitudes that  
 308 may help increasing slightly the recognition rate. Maybe the classifier is using  
 309 specific vibration pattern of each key, wave reflections inside the device or some  
 310 other complex phenomena to improve the key classification rate. If we use four  
 311 features, the recognition rate decreases to 96.5%.

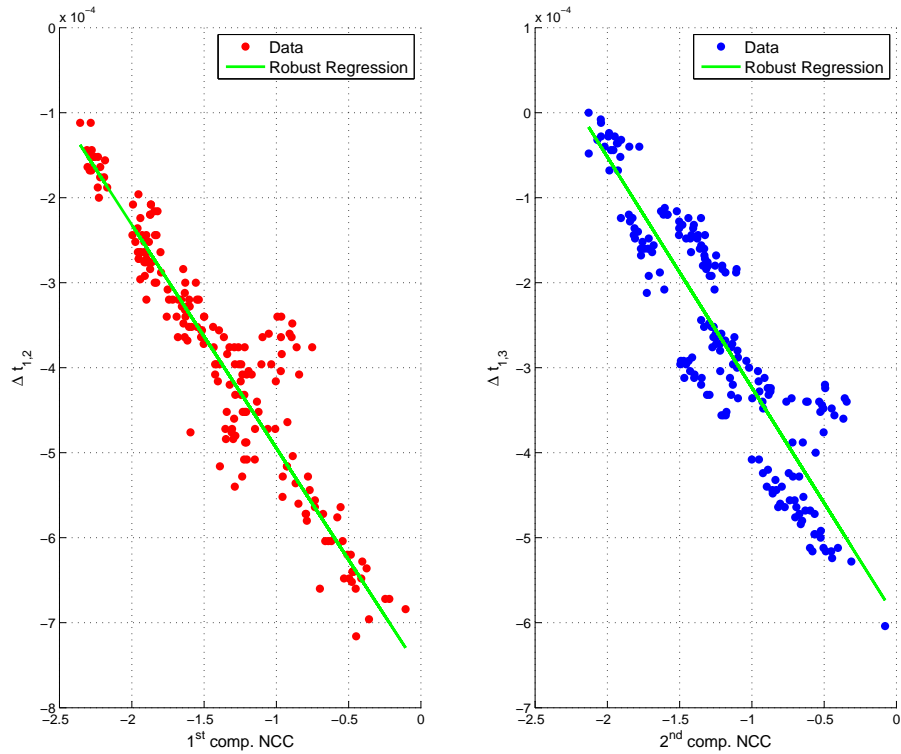


Figure 10: Comparison between the two main NCC-PCA components and the two TDOA features (the delays between the vibration signals). The pairs of features computed in different ways are highly correlated.

### 312 4.3. PCI Requirements

313 PCI requires that an attack such as described in this work should be pos-  
 314 sible only with very high cost of 26 for identification and 13 for exploitation<sup>2</sup>.  
 315 Nevertheless, the vibration delay attack to this PCI-PTS compliant equipment  
 316 costs only 12.5 for identification and 3.5 for exploitation (Table 3). The method

---

<sup>2</sup> “There is no feasible way to determine any entered and internally transmitted PIN digit by monitoring sound, electro-magnetic emissions, power consumption or any other external characteristic available for monitoring – even with the cooperation of the device operator or sales clerk – without requiring an attack potential of at least 26 for identification and initial exploitation with a minimum of 13 for exploitation.” [20, p. 16]

Table 3: Calculation of the Cost of PIN-pad Vibration Delay Attack

Factor	Identification	Exploitation
Attack time	Beyond 160 hours = 5.5	≤1 hour = 0
Expertise	Expert = 4	Layman = 0
Knowledge of the PIN entry device	Public = 0	Public = 0
Access to the PIN entry device	Mechanical Sample = 1	Mechanical Sample = 1
Equipment required for the attack	Standard = 1	Standard = 1
Specific parts required	Standard = 1	Standard = 1
<b>Total cost</b>	<b>12.5</b>	<b>3</b>

Table 4: Comparisons between the Main Experiments

	Previous work		This work
	ATM	PIN2 rigid	PIN-pad
Features per keystroke	63	165	3
Accelerometers	3	2	3
Success rate	98.4%	76.7%	96.4%

317 used to calculate the costs can be found in [20, p. 142].

## 318 5. Considerations

319 Table 4 compares the main experiments of our previous work [2] and of this  
 320 work. Clearly, “PIN2 rigid mode” experiment of the previous work has the lowest  
 321 success rate. As we now know the main physical phenomenon for leaking the  
 322 information, we can explain the cause for this low rate. It is because in that  
 323 experiment we used only two accelerometers. Thus, TDOA cannot uniquely  
 324 determine the location of the vibration source.

325 The success rate of the ATM experiment of our previous work is slightly  
 326 higher than PIN-pad experiment of this work. The recognition rates of the  
 327 two experiments cannot be compared directly, because they are attacking two  
 328 different devices (ATM keypad and PIN-pad). However, as we said in the last  
 329 Section, it seems that there are other information (besides TDOA) in NCC  
 330 amplitudes that may increase slightly the recognition rate.

## 331 6. Conclusion

332 In this paper, we have demonstrated that the primary cause that makes  
333 it possible to identify the pressed key by monitoring the vibrations with ac-  
334 celerometers is the relative delays in the wavefront arrival times at different  
335 accelerometers located at different points. We have shown that the propagation  
336 delay of the wavefront generated by the keystroke makes each accelerometer  
337 feel similar vibrations at different moments. These relative delays is used in our  
338 “vibration delay attack”. A simple classification scheme using the relative delays  
339 yielded 96.4% of key recognition success rate.

340 We also have shown that a PIN-pad, a device properly designed to counter  
341 side-channel attacks and PCI-PTS compliant is very vulnerable to the vibration  
342 delay attack. Clearly, the vibration delay attack can also be applied to touch  
343 screen devices.

344 Our finding indicates (i) the care that an engineer must have to design secure  
345 human-machine interface devices in the future and (ii) a new attack vector that  
346 certification processes must address hereafter.

## 347 Appendix A. Normalized cross correlation

348 Let the vector  $v$  with elements  $v_i$ ,  $0 \leq i < N$  represent the acceleration  
349 values captured by an accelerometer. The mean-corrected vector  $\tilde{v}$  has elements  
350  $\tilde{v}_i = v_i - \bar{v}$ , where  $\bar{v}$  is the mean of  $v$ . We use only mean-corrected acceleration  
351 values, because we are not interested in the static acceleration of gravity. The  
352 correlation coefficient between the two mean-corrected vectors is:

$$corr(\tilde{v}, \tilde{w}) = \frac{\tilde{v} \cdot \tilde{w}}{\|\tilde{v}\| \|\tilde{w}\|} \quad (\text{A.1})$$

353 Correlation coefficient measures the “similarity” between the two vectors, invari-  
354 ant to bias (because the vectors are mean-corrected) and to gain (because the  
355 vectors are divided by their norms).

Normalized cross correlation (NCC) between vectors  $v$  and  $w$  is a vector de-  
noted as  $\tilde{v} \otimes \tilde{w}$  whose elements are the correlation coefficients computed between

time-shifted vectors, ignoring the elements that do not have the matching pair.

It has  $2N - 1$  elements:

$$(\tilde{\mathbf{v}} \otimes \tilde{\mathbf{w}})_n = \begin{cases} \frac{\sum_{i=0}^{N-n-1} \tilde{v}_i \tilde{w}_{n+i}}{\sqrt{\sum_{i=0}^{N-n-1} \tilde{v}_i^2 \sum_{i=0}^{N-n-1} \tilde{w}_{n+i}^2}}, & 0 \leq n < N & \text{(A.2a)} \\ (\tilde{\mathbf{w}} \otimes \tilde{\mathbf{v}})_{-n}, & -N < n < 0 & \text{(A.2b)} \end{cases}$$

356 Note that  $(\tilde{v} \otimes \tilde{w})_0 = \text{corr}(\tilde{v}, \tilde{w})$ . NCC has been used for a long time in com-  
 357 puter vision to find templates in search images, in an operation called template  
 358 matching. We use Matlab function `xcov(v,w,'coeff')` to compute NCC.

## 359 Appendix B. Source location estimation

360 We present here the technique used to estimate the positions of keys through-  
 361 out this paper. Note that it is not necessary to know the spatial position of the  
 362 pressed key in order to identify it. We suppose that the group velocity is con-  
 363 stant throughout the device and consequently that the relative distances are  
 364 roughly equivalent to the measured relative delays. For instance, we consider  
 365 that the distance  $d_1 - d_2$  is approximately equal to the measured relative delay  
 366  $\Delta t_{1,2}$  between accelerometers  $A_1$  and  $A_2$  (Fig. B.11). Similarly, we assume that  
 367  $d_1 - d_3 \approx \Delta t_{1,3}$  and  $d_2 - d_3 \approx \Delta t_{2,3}$ .

368 The following reasoning demonstrates that only two time differences carry  
 369 useful information. Consider  $\Delta t_{1,2} = t_1 - t_2$ . Doing the same for  $\Delta t_{1,3}$  and  
 370  $\Delta t_{2,3}$ , it is easy to see that  $\Delta t_{2,3} = \Delta t_{1,3} - \Delta t_{1,2}$ , a linear combination of the  
 371 other two features, not carrying new information.

372 We estimate the source location  $P$  by a simple numerical optimization, using  
 373 Matlab function `fminunc`. We minimize the following functional:

$$f = c_{1,2} + c_{1,3}. \quad \text{(B.1)}$$

where  $c_{1,2}$  is:

$$c_{1,2} = \begin{cases} [d_1^2 - (d_2 + \Delta t_{1,2})^2]^2, & \Delta t_{1,2} \geq 0 & \text{(B.2a)} \\ [d_2^2 - (d_1 + \Delta t_{1,2})^2]^2, & \Delta t_{1,2} < 0. & \text{(B.2b)} \end{cases}$$

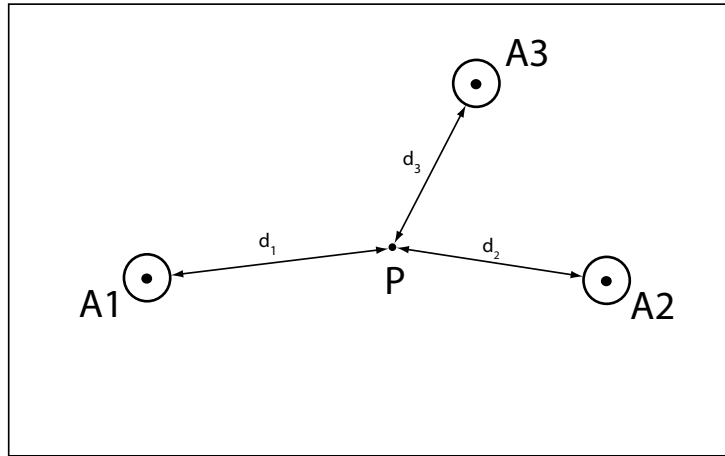


Figure B.11: Diagram of trilateration method.

374 The cost  $c_{1,3}$  is defined similarly. The distance  $d_i$  from the accelerometer  
 375  $A_i = (A_i^x, A_i^y)$  to the point  $P = (P^x, P^y)$  is:

$$d_i = \|A_i - P\| = \sqrt{(A_i^x - P^x)^2 + (A_i^y - P^y)^2} \quad (\text{B.3})$$

376 If we substitute Eq. B.2 and B.3 in Eq. B.1 and minimize  $f$ , we get the  
 377 approximate position of point  $P$  (Fig. B.11).

### 378 References

- 379 [1] Verizon, Verizon 2014 Data Breach Investigations Report (2014).  
 380 URL <http://www.verizonenterprise.com/DBIR/2014/>
- 381 [2] G. de Souza Faria, H. Y. Kim, Identification of pressed keys from mechan-  
 382 ical vibrations, Information Forensics and Security, IEEE Transactions on  
 383 8 (7) (2013) 1221–1229. doi:10.1109/TIFS.2013.2266775.
- 384 [3] A. Tarantola, Inverse Problem Theory and Methods for Model Parameter  
 385 Estimation, Society for Industrial and Applied Mathematics, 2005. arXiv:  
 386 <http://epubs.siam.org/doi/pdf/10.1137/1.9780898717921>, doi:10.  
 387 1137/1.9780898717921.  
 388 URL <http://epubs.siam.org/doi/abs/10.1137/1.9780898717921>

- 389 [4] D. Asonov, R. Agrawal, Keyboard acoustic emanations, in: Security and  
390 Privacy, 2004. Proceedings. 2004 IEEE Symposium on, 2004, pp. 3–11.  
391 doi:10.1109/SECPRI.2004.1301311.
- 392 [5] Y. Berger, A. Wool, A. Yeredor, Dictionary attacks using keyboard acoustic  
393 emanations, in: In Proceedings of Computer and Communications Security  
394 (CCS, 2006.
- 395 [6] L. Zhuang, F. Zhou, J. D. Tygar, Keyboard acoustic emanations revis-  
396 ited, ACM Trans. Inf. Syst. Secur. 13 (1) (2009) 3:1–3:26. doi:10.1145/  
397 1609956.1609959.  
398 URL <http://doi.acm.org/10.1145/1609956.1609959>
- 399 [7] T. Halevi, N. Saxena, A closer look at keyboard acoustic emanations: Ran-  
400 dom passwords, typing styles and decoding techniques, in: Proceedings  
401 of the 7th ACM Symposium on Information, Computer and Communica-  
402 tions Security, ASIACCS '12, ACM, New York, NY, USA, 2012, pp. 89–90.  
403 doi:10.1145/2414456.2414509.  
404 URL <http://doi.acm.org/10.1145/2414456.2414509>
- 405 [8] P. Marquardt, A. Verma, H. Carter, P. Traynor, (sp)iphone: Decoding  
406 vibrations from nearby keyboards using mobile phone accelerometers, in:  
407 Proceedings of the 18th ACM Conference on Computer and Communica-  
408 tions Security, CCS '11, ACM, New York, NY, USA, 2011, pp. 551–562.  
409 doi:10.1145/2046707.2046771.  
410 URL <http://doi.acm.org/10.1145/2046707.2046771>
- 411 [9] M. Ge, Analysis of source location algorithms - part i: Overview and non-  
412 iterative methods, J. Acoustic Emission 21.  
413 URL <http://www.ndt.net/article/jae/papers/21-014.pdf>
- 414 [10] M. Ge, Analysis of source location algorithms - part ii: Iterative methods,  
415 J. Acoustic Emission 21.  
416 URL <http://www.ndt.net/article/jae/papers/21-029.pdf>

- 417 [11] K. Ho, Y. Chan, Solution and performance analysis of geolocation by tdoa,  
418 Aerospace and Electronic Systems, IEEE Transactions on 29 (4) (1993)  
419 1311–1322. doi:10.1109/7.259534.
- 420 [12] F. Gustafsson, F. Gunnarsson, Positioning using time-difference of arrival  
421 measurements, in: Acoustics, Speech, and Signal Processing, 2003. Pro-  
422 ceedings. (ICASSP '03). 2003 IEEE International Conference on, Vol. 6,  
423 2003, pp. VI-553–6 vol.6. doi:10.1109/ICASSP.2003.1201741.
- 424 [13] D. Manolakis, Efficient solution and performance analysis of 3-d position  
425 estimation by trilateration, Aerospace and Electronic Systems, IEEE Trans-  
426 actions on 32 (4) (1996) 1239–1248. doi:10.1109/7.543845.
- 427 [14] T. Schumacher, D. Straub, C. Higgins, Toward a probabilistic  
428 acoustic emission source location algorithm: A bayesian approach,  
429 Journal of Sound and Vibration 331 (19) (2012) 4233 – 4245.  
430 doi:http://dx.doi.org/10.1016/j.jsv.2012.04.028.  
431 URL [http://www.sciencedirect.com/science/article/pii/  
432 S0022460X12003446](http://www.sciencedirect.com/science/article/pii/S0022460X12003446)
- 433 [15] K. Arun, E. Ong, A. Khong, Source localization on solids using kullback-  
434 leibler discrimination information, in: Information, Communications and  
435 Signal Processing (ICICS) 2011 8th International Conference on, 2011, pp.  
436 1–5. doi:10.1109/ICICS.2011.6174299.
- 437 [16] W. Elmore, M. A. Heald, Physics of Waves, Dover, 1969.
- 438 [17] L. Meirovitch, Analytical Methods in Vibrations, Macmillan, 1967.
- 439 [18] Freescale Semiconductor - MMA7361LC:  $\pm 1.5g$ ,  $\pm 6g$ , 3-Axis Analog  
440 Output Acceleration Sensor (February 2015).  
441 URL [http://www.freescale.com/webapp/sps/site/prod\\_summary.  
442 jsp?code=MMA7361LC](http://www.freescale.com/webapp/sps/site/prod_summary.jsp?code=MMA7361LC)



- 443 [19] G. S. Faria, H. Y. Kim, Identificação das teclas digitadas a partir da vi-  
444 bração mecânica, in: Anais do 30º Simpósio Brasileiro de Telecomunicações  
445 - SBrT, 2012.
- 446 [20] Payment Card Industry - Security Standards Council LLC, PIN Trans-  
447 action Security (PTS) Point of Interaction (POI) Modular Derived Test  
448 Requirements v4.0 (June 2013).